RKKY-like contributions to the magnetic anisotropy energy: 3*d* adatoms on Pt(111) surface

Mohammmed Bouhassoune,[*] Manuel dos Santos Dias, Bernd Zimmermann, Peter H. Dederichs, and Samir Lounis[†]

Peter Grünberg Institut and Institute for Advanced Simulation, Forschungszentrum Jülich and JARA, D-52425 Jülich, Germany

The magnetic anisotropy energy defines the energy barrier that stabilizes a magnetic moment. Utilizing density-functional-theory-based simulations and analytical formulations, we establish that this barrier is strongly modified by long-range contributions very similar to Friedel oscillations and Rudermann-Kittel-Kasuya-Yosida interactions. Thus, oscillations are expected and observed, with different decaying factors and highly anisotropic in realistic materials, which can switch nontrivially the sign of the magnetic anisotropy energy. This behavior is general, and for illustration we address the transition-metal adatoms, Cr, Mn, Fe, and Co deposited on a Pt(111) surface. We explain, in particular, the mechanisms leading to the strong site dependence of the magnetic anisotropy energy observed for Fe adatoms on a Pt(111) surface as revealed previously via first-principles-based simulations and inelastic scanning tunneling spectroscopy [A. A. Khajetoorians *et al.*, Phys. Rev. Lett. **111**, 157204 (2013)]. The same mechanisms are probably active for the site dependence of the magnetic anisotropy energy obtained for Fe adatoms on Pd or Rh(111) surfaces and for Co adatoms on a Rh(111) surface [P. Blonski *et al.*, Phys. Rev. B **81**, 104426 (2010)].

I. INTRODUCTION

As magnetic devices shrink toward atomic dimensions, with the ultimate goal of encoding information in the smallest possible magnetic entity, the understanding of magnetic stability down to the single-atomic limit becomes crucial. Here, a critical ingredient is the magnetic anisotropy energy (MAE), which provides directionality and stability to magnetization. The higher the MAE, the more protected is the magnetic bit against, for example, thermal fluctuations. Thus the search for nanosystems with enhanced MAE is a very active field, giving the perspective of stabilizing and simultaneously reducing the size of magnetic bits.

Recently, it was demonstrated that nanostructures with only a few atomic spins, ranging from single atoms, to clusters on metal surfaces (see, for example, Refs. [1–10]), to molecular magnets (e.g., Refs. [11–14]), can exhibit MAEs that are large enough to maintain, in principle, a stable spin orientation at low temperatures. A celebrated example is the giant MAE ($\sim$9 meV) discovered by Gambardella *et al.* [1] for a single Co adatom on Pt(111) surface. There the right ingredients for a large MAE are satisfied: a large magnetic moment carried by the 3*d* transition element, Co, being at the vicinity of heavy substrate atoms characterized by a large spin-orbit interaction (SOI). Naturally, here details of the electronic structure and hybridization effects are decisive. Thus exchanging the Co adatom for an Fe adatom leads to an extremely low MAE as demonstrated recently by inelastic scanning tunneling spectroscopy and *ab initio* simulations based on density functional theory (DFT) [15]. Most intriguing in the latter work is the dramatic change in the MAE magnitude and sign once the Fe adatom is moved from an *fcc* stacking site, where the moment points out-of-plane, to an *hcp* stacking site, where the moment lies in-plane. This was assigned to the proximity effect, leading to a large spin

polarization cloud induced by Fe in the Pt substrate, which is notorious for its high magnetic polarizability [16,17] as seen also for Pd [18–22]. A similar site-dependent MAE for Fe adatoms on the (111) surfaces of Pd and Rh and for Co on Rh(111) was noted with *ab initio* simulations [23]. The physical mechanism behind such behavior has not been, to our knowledge, identified convincingly. Even on surfaces with a low polarizability, such as gold, the MAE follows an oscillating behavior depending on the distance to the surface of buried magnetic nanostructures [24–26]. Thus the polarizability is probably not the only ingredient modifying the strength of the MAE since Au is much less polarizable than Pt. One must keep in mind that the polarizability of the substrate atoms is determined by the Stoner product $I \cdot N_F$, with the exchange integral I and the number of states at the Fermi level N_F ($I \cdot N_F = 0.29$ for Ir, 0.59 for Pt, and 0.05 for Au) [27].

The goal of our work is to demonstrate with a formal proof that a strong contribution to the MAE can be highly nonlocal and long-ranged and may contribute up to $\pm 50\%$ of the total MAE. Strong similarities can be foreseen with respect to Friedel [28] and Rudermann-Kittel-Kasuya-Yosida (RKKY) [29] oscillations in terms of the impact of the nature of the mediating electronic states, their localization in real space, and their shape in reciprocal space (e.g., Fermi surface) on the decay of the oscillations and their focusing (see, e.g., Refs. [17,30–39]). A particularity of this long-range contribution to the MAE is, as expected, its dependence on the strength of the SOI. Taking as an illustration 3*d* adatoms (Cr, Mn, Fe, and Co) deposited on a Pt(111) surface, we demonstrate that the contribution of the substrate Pt atoms to the total MAE oscillates and decays with their distance to the adatom.

II. METHOD

The MAE can be determined from the magnetic force theorem [40,41], taking the energy difference, $\epsilon_\perp - \epsilon_{||}$, between the band energies of the two configurations: out-of-plane ($\perp$) and in-plane ($||$) orientations of the magnetic moment. A reference magnetic configuration is chosen, here the out-of-plane

---

[*]m.bouhassoune@fz-juelich.de
[†]s.lounis@fz-juelich.de

orientation, where the self-consistent calculations are performed and the related band energy is obtained. Then the magnetic moment is rotated in-plane and one iteration is done in order to extract the band energy. With such a traditional technique, one reduces the error made by taking differences between the total energies, which are large numbers. A positive sign of the MAE indicates an in-plane preferable orientation of the adatom's magnetic moment. We utilize the full potential relativistic Korringa-Kohn-Rostoker Green function (FP-KKR-GF) method [42,43]. The local spin density approximation as parametrized by Vosko, Wilk, and Nusair was used [44]. First, the electronic structure of a 22-layer Pt slab with two additional vacuum regions (8 layers) was calculated. The experimental lattice parameter (3.92 Å) was considered without surface relaxations, which are negligible [45]. Then each adatom is embedded on the surface of this slab, in real space, together with its neighboring sites, defining a cluster of atoms, where the charge is allowed to be updated during self-consistency. We note that the cluster still interacts with the rest of the host surface via the Coulomb interaction. The adatoms are allowed to relax towards the surface, and we found qualitatively a similar behavior for the magnetic moments and the MAE in the range of relaxation from 15% to 25% towards the surface. As indicated in Ref. [15], Fe was found to relax by 20% towards the surface. The same relaxed geometry was found for Co adatoms [46]. Thus for the sake of comparison, the four investigated adatoms were assumed to be at the same relaxed position 20% towards the surface. The MAE is extracted for clusters of different sizes, for which the Green functions of the impurity-free surface are generated with $200 \times 200\,k$ points in the two-dimensional Brillouin zone and a maximum angular quantum number $l = 3$. To provide an idea of the convergence of the MAE versus the number of k points we address the case of an Fe adatom in contact with a Pt substrate, where 221 Pt atoms are allowed to be perturbed by the impurity. The MAE is found to change by about 0.002% with respect to the one obtained for $200 \times 200\,k$ points when the number of k points is decreased to 180×180 or 150×150.

III. RESULTS AND DISCUSSION

A. Fe adatoms, *fcc* versus *hcp* stacking sites

Figure 1 displays the MAE obtained with the band energy differences of an Fe adatom sitting at an *fcc* or an *hcp* site on a Pt(111) surface versus the number of Pt atoms included in the real-space calculations. This figure is included in the Supplemental Material to Ref. [15]. If only the nearest-neighbor (NN) Pt atoms to the Fe impurity are considered, in this case three Pt atoms, the MAE yields an out-of-plane easy axis with the same value of −2.8 meV for both binding sites. However, considering more Pt atoms, the neighborhoods of the two stacking sites differ, and therefore the MAE becomes strongly dependent on the binding site and even changes sign for the *hcp* site. The latter occurs when 16 Pt atoms are included in the surrounding cluster in addition to the NN atoms. The MAE first decreases from −2.8 to −3.3 meV upon the inclusion of the 10 closest Pt neighboring atoms and then, surprisingly, jumps to +0.1 meV upon the addition of the more distant 6 Pt atoms [blue in Figs. 2(a) and 2(b)]. The latter means that these
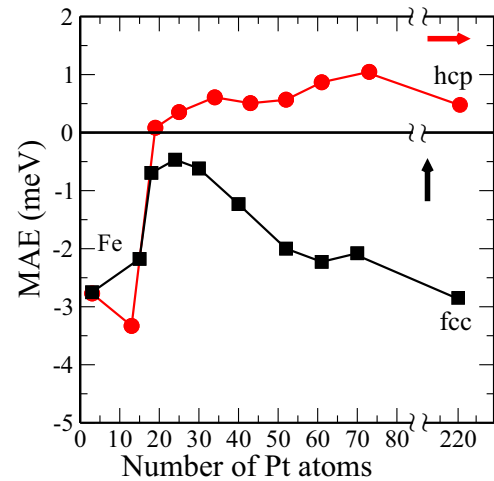

FIG. 1. MAE of an Fe impurity adsorbed at an *fcc* (square) or an *hcp* (circle) site on a Pt(111) surface versus the number of Pt atoms in the cluster. A positive MAE corresponds to an in-plane orientation of the magnetic moment and a negative MAE corresponds to an out-of-plane magnetic moment. (Readapted from Supplemental Fig. 3 of Ref. [15].)

six Pt atoms, with their positive contribution (+3.4 meV) to the MAE, play a key-in switching the preferable orientation of the adatom's magnetic moment. These *switcher* atoms are equivalent, belong to the subsurface layer, and are equidistant (∼0.5 nm) from the adatom. Interestingly, the switcher atoms occur also for the *fcc* binding site and are located similarly to the *hcp* binding site, at the subsurface layer equidistant from the adatom. However, their number is lower than in the *hcp* stacking site: three instead of six [see Figs. 2(c) and 2(d)]. Therefore, their contribution to the MAE (+1.5 meV) is about half their contribution for the *hcp* binding site. This is not sufficient to compete against the preferable orientation of the
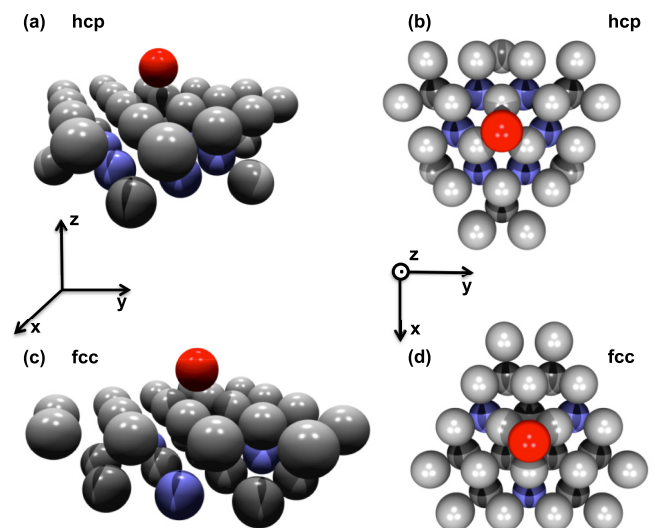

FIG. 2. Atomic structures of Fe impurity adsorbed on an *hcp* site [(a) side view and (b) top view] or an *fcc* site [(c) side view and (d) top view] of a Pt(111) surface. Pt atoms (blue) are the switching atoms, which make a large contribution to the MAE.
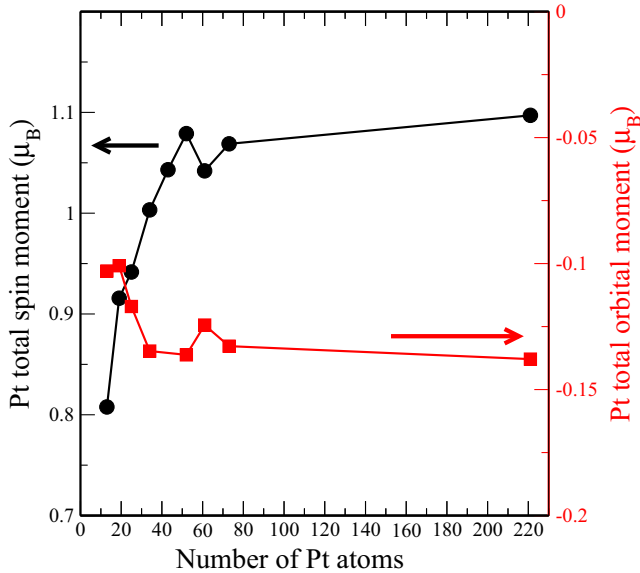
FIG. 3. Convergence of the total *z* component of the spin moment and orbital moment induced in Pt atoms of different cluster sizes. The cases of Fe adatoms sitting at *hcp* or *fcc* binding sites are considered and the *z* direction is perpendicular.

TABLE I. Total magnetic spin and orbital moments of the Fe adatom including different sets of neighboring Pt atoms. The total spin moment (m_s) converges after 53 Pt atoms are considered, while the total orbital moment (m_{orb}) is already saturated with nearest-neighbor Pt atoms.

No. of	Fe *hcp*		Fe *fcc*	
Pt atoms	m_s	m_{orb}	m_s	m_{orb}
3	4.11	0.22	4.03	0.23
53	4.57	0.216	4.427	0.227
221	4.59	0.21	4.42	0.212

adatom and its NNs (MAE $= -2.8$ meV). Indeed, when the switching atoms are included the MAE jumps from -2.2 meV, obtained with a cluster containing 15 Pt atoms, to -0.7 meV. After the addition of more substrate atoms, reaching a cluster of $\sim$221 atoms, the MAE tends to $+0.5$ and -2.9. meV for the *hcp* and *fcc* binding sites, respectively. The latter values are rather converged since smaller clusters with a number of atoms (not shown in Fig. 1) close to the largest one show a stable MAE.

We have also examined the effect of the Pt polarization cloud on the total spin and orbital magnetic moments. Interestingly, the impact on the total moment is less impressive than that on the MAE as summarized in Table I for the case of the Fe adatom with a magnetic moment pointing out-of-plane. When only the NN Pt atoms are included the total spin moment reaches a value of $\sim 4\mu_B$, while the total orbital moment is around $0.2\mu_B$. The inclusion of a larger number of neighboring Pt atoms increases the total spin moment by a maximum of $\sim 0.4\mu_B$, while the total orbital moment reaches saturation already with the NN atoms. This observation can be extracted from Fig. 3, where the induced Pt total *z* components of the spin and orbital moments are plotted for the case where the impurity sits at the *hcp* stacking site. The *z* direction is perpendicular to the substrate.

As a summary, one realizes that the contributions of the different Pt shells to the total MAE is not uniform, oscillates with the distance, and certainly does not correlate perfectly with the change in the total spin moment or total orbital moment. The latter quantities describe the polarization of the Pt cloud. At first sight, one could ask whether Fig. 1 is the result of numerical artifacts related to the KKR embedding scheme. In principle, whenever a cluster is considered, the atoms sitting at the edge of the cluster will feel the boundary conditions more strongly than the atoms close to the Fe impurity. As

illustrated in Fig. 4, the edge atoms are not that affected by the boundary conditions. The spread of the plotted values gives an idea of the impact of the cluster size on the individual Pt magnetic moments. As an example, the spin moment of the edge atom, located at $\sim$0.65 nm, in the cluster containing 34 atoms is on top of the spin moment of the same Pt atom when the boundary conditions have been improved by extending the size of the cluster to 220 Pt atoms. The same conclusion can be drawn for the orbital moment, although here the values are much smaller than the spin moments. In general, the boundary conditions will affect slightly the values obtained for the magnetic properties including the MAE. However, the general oscillatory behavior shown in Fig. 1 seems to go beyond the numerical conditions needed to extract it. The main reason is that the Pt spin moment, for instance, has two contributions: induced either by the magnetic adatom or by the surrounding magnetic Pt atoms. The former makes, in general, a much stronger contribution than the latter. Also, within the KKR embedding scheme the atoms at the edge feel the Coulomb interaction of the neighboring atoms beyond the cluster.

In the following the origin of the oscillatory behavior of the MAE is discussed by realizing that the band energies, ϵ, can be evaluated from $-\int_{-\infty}^{E_F} dE\,N(E)$, i.e., an integration up to the Fermi energy, E_F, of the integrated density of states (IDOS), $N(E)$, which in turn can be extracted from the celebrated Lloyd's formula [47]. Indeed, if a system described by a Green function, G, is perturbed by a potential V, the change in the IDOS, $\delta N(E)$, is given simply by $-\frac{1}{\pi}\Im\text{Tr}\ln(1 - VG(E))$, where the trace is taken over the site index and orbital and spin angular momentum quantum numbers. This permits the aforementioned decomposition of the MAE into local and nonlocal contributions by wise evaluation of the change in the IDOS.

B. Long-range contributions to the MAE: Formalism and results

First, we note that once the adatom is deposited on a substrate, it strongly perturbs the potentials of the NN Pt atoms, i.e., three Pt atoms in total. If we consider solely the adatom and its NN Pt atoms, the corresponding Green function, G_1, can be obtained from the Dyson equation

$$G_1(E) = G_0(E) + G_0(E)V_1 G_1(E), \qquad (1)$$

where G_0 is the Green function of the ideal surface of Pt without an SOI, while V_1 is the perturbing potential limited
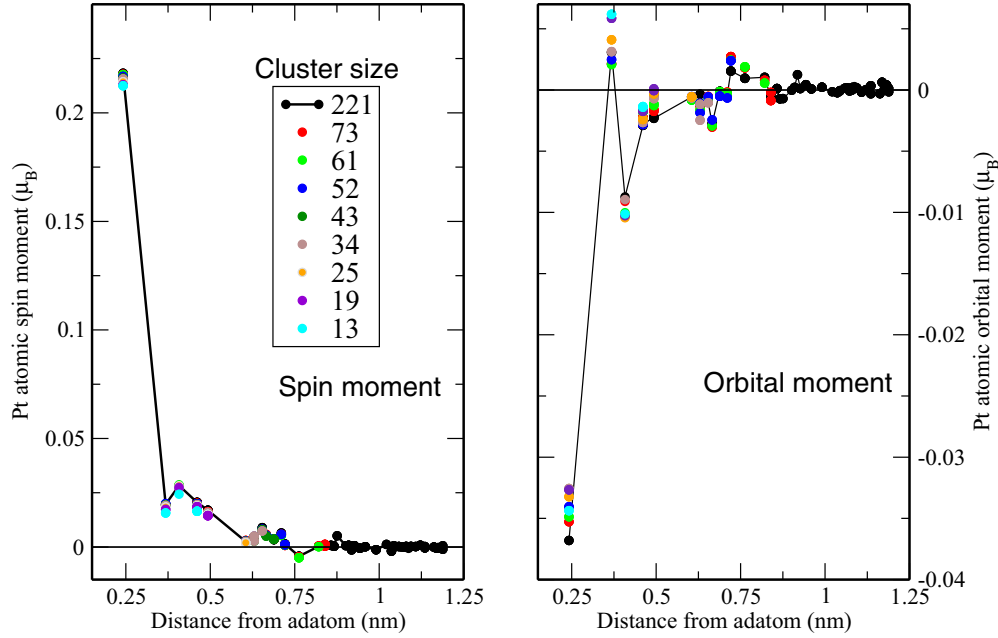
FIG. 4. The individual Pt atomic spin moment (left) and orbital moment (right) as a function of the distance with respect to an Fe adatom sitting at an *hcp* binding site. The spread of the magnetic moments for the different cluster sizes is rather small, highlighting the low impact of the boundary conditions of KKR simulations on these magnetic properties.

to the region of the adatom and its NN and is induced by the presence of the impurity and the SOI. Instead of the potential V_1, one can use the scattering matrix T_1:

$$G_1(E) = G_0(E) + G_0(E)T_1(E)G_0(E). \quad (2)$$

From the previous Dyson equations, the local electronic and magnetic properties of the adatom can be reasonably described. For instance, it leads to an MAE of -2.8 meV for the Fe adatom. To grasp the effect of the rest of the Pt atoms, i.e., the hundreds of outer Pt atoms, on the MAE, we solve a second Dyson equation to obtain the new Green function, G_2,

$$G_2(E) = G_1(E) + G_1(E)V_2G_2(E), \quad (3)$$

where the perturbing potential, V_2, describes simultaneously the change induced by the adatom in the additionally incorporated 217 outer Pt atoms (V_2') and their SOI (V_2^{so}). In fact, $V_2^{so} = \xi(E)\mathbf{L} \cdot \mathbf{S}$, with $\xi(E)$ being the strength of the SOI. Thus, $V_2 = \sum_j(V_{2j}' + V_{2j}^{so})$, where the sum runs over all outer Pt atoms. In contrast to T_1, V_2 is limited to the rest of the Pt atoms and is expected to be relatively small since the perturbation decays with the distance from the adatom, which permits the use of Taylor expansions when solving Eq. (3).

The change in the IDOS, $\delta N(E)$, due to the coupling of the adatom and its NN to the rest of the Pt substrate atoms, is then given as $-\frac{1}{\pi}\Im\mathrm{Tr}\ln(1 - V_2G_1(E))$, which for small V_2 can be expanded up to second order:

$$\delta N(E) = \frac{1}{2\pi}\Im\mathrm{Tr}[2V_2G_1(E) + V_2G_1(E)V_2G_1(E)]. \quad (4)$$

We express G_1 in terms of G_0 as given in Eq. (2), drop terms leading to third- and fourth-order processes (these are expected to be much smaller than the second order-processes), and find

$$\delta N = \frac{1}{2\pi}\Im\mathrm{Tr}[2V_2G_0 + 2V_2G_0T_1G_0 + V_2G_0V_2G_0], \quad (5)$$

where the energy argument, E, was taken out for the sake of simplicity. Since V_2 is written in terms of non-SOI- and SOI-dependent terms, this allows us to disentangle the previous expression:

$$\delta N = \frac{1}{\pi}\Im\mathrm{Tr}\sum_j \left\{ V_{2j}'G_0 + V_{2j}^{so}G_0 \right.$$
$$+ T_1G_0V_{2j}'G_0 + T_1G_0V_{2j}^{so}G_0$$
$$\left. + \frac{1}{2}\sum_{j'}(V_{2j}' + V_{2j}^{so})G_0(V_{2j'}' + V_{2j'}^{so})G_0 \right\}. \quad (6)$$

In view of our interest in the band energies, which depend on the rotation of the magnetic moment, i.e., contributing to the MAE, not all terms in Eq. (6) are relevant. For instance, the term of first order in V_2 or G_0 contains either no spin-orbit coupling or only the linear SOI term. Therefore they vanish when one evaluates the MAE. From the last term, only the contribution from the scattering at V_2' and at V_2^{so} is finite. Since these atoms are only weakly spin polarized, the latter term is negligible as verified numerically and therefore it is not considered in the following. The contribution to the band energy relevant for the MAE is then given by

$$-\frac{1}{\pi}\Im\mathrm{Tr}\int_{-\infty}^{E_F} dE \sum_j \left\{ T_1G_0V_{2j}'G_0 + T_1G_0V_{2j}^{so}G_0 \right\}, \quad (7)$$

which has to be evaluated at the different configuration $\perp$ and $||$ orientations of the magnetic moment in order to extract the MAE.

The first term is the simplest. It is independent of the SOI of the outer Pt atoms and just describes a renormalization of the MAE of the small cluster consisting of the Fe atoms and the three Pt atoms due to the scattering at the potentials

V'_{2j} of the outer Pt atoms, which does not include the SOI of these atoms. Therefore we call this contribution the no-so term. The second term, called the so term, is also important and describes the double scattering at the SOI term of T_1 and the SOI potential V^{so}_{2j} of the outer atoms. These two terms might therefore be described as nonlocal, since they connect the scattering at the SOI of the inner cluster with the scattering at the potentials of the outer atoms. The analogy of these nonlocal terms with the celebrated formula from Lichtenstein *et al.* [48,49] for the evaluation of the magnetic exchange interactions is appealing, and as for the magnetic interactions, we expect these two terms to oscillate and decay with the

distance between the two regions. Instead of the magnetic part of the potential, the scattering occurs at the SOI term, but the mediation is made in both cases via the Green functions.

In order to clarify the importance of the nonlocal terms in the MAE, we have therefore recalculated the anisotropy by switching on and off the SOIs of individual outer Pt atoms, based on Eq. (7). In this way, we demonstrate how the relatively small so and no-so contributions of an outer Pt atom change the MAE of a complex system containing an Fe atom, its NN, and the preselected outer Pt atom and show Friedel-like oscillations. For this analysis, the cluster thus contains an Fe adatom, its three NN Pt atoms, and one
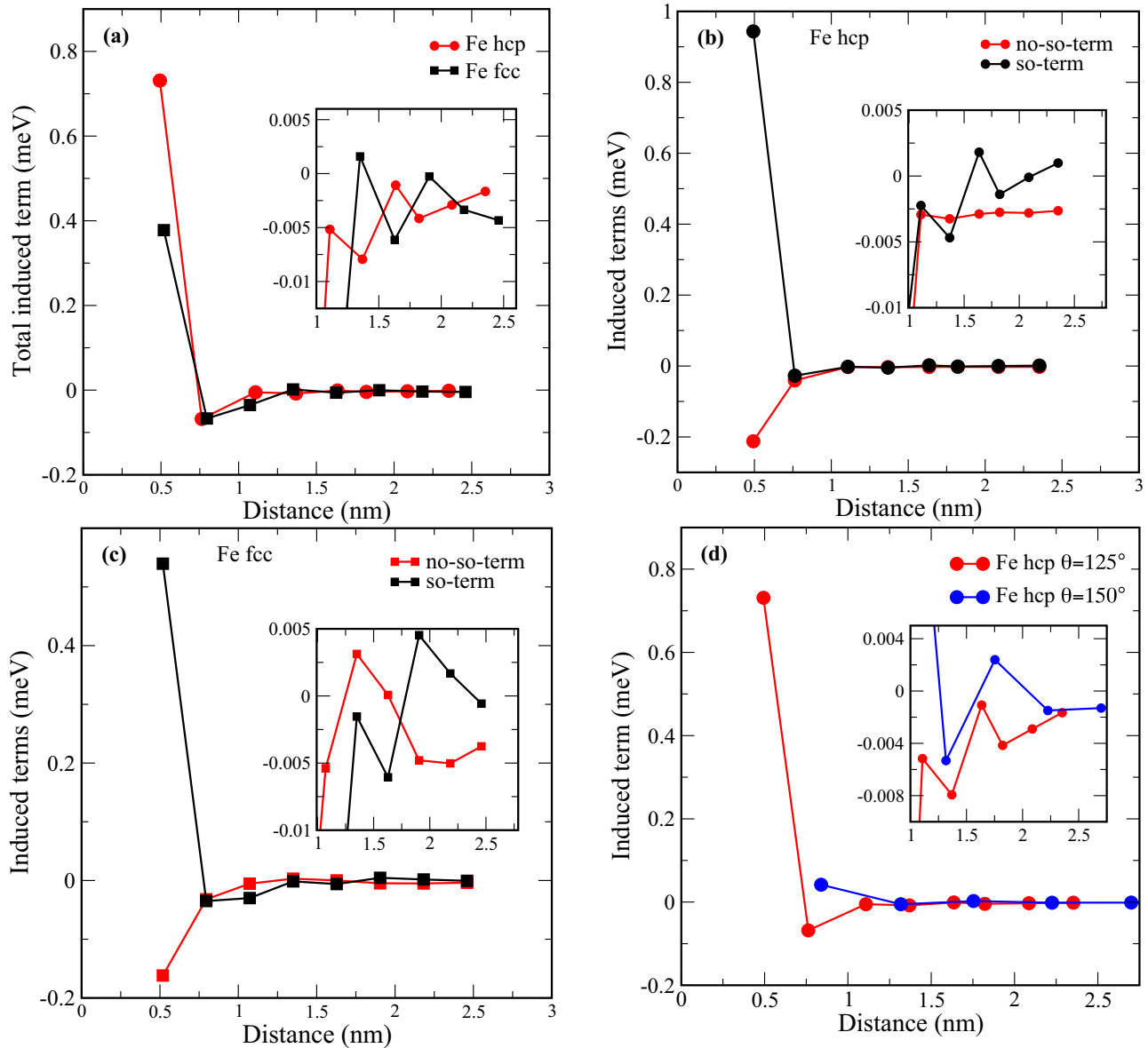

FIG. 5. Contributions to the MAE from different shells of Pt atoms versus their distance with respect to the adatom sitting either at an *fcc* or at an *hcp* stacking site. (a–c) The plotted values correspond to Pt atoms sitting along the direction connecting the adatom with one of the switching Pt atoms, i.e., ($\theta = 125°$, $\phi = -60°$) for the *hcp* stacking site and ($\theta = 128°$, $\phi = 30°$) for the *fcc* stacking site. Inset: Enhancement of the oscillations observed in nonlocal terms. While in (a) the sum of the nonlocal contributions to the MAE is plotted, in (b) and (c) the no-so and so terms are plotted separately for the *hcp* and *fcc* sites, respectively. (d) Anisotropy of the nonlocal contribution to the MAE obtained for two sets of angles: ($\theta = 125°$, $\phi = -60°$) compared to ($\theta = 150°$, $\phi = 80°$). The magnitude of the MAE is clearly more enhanced along the direction passing by the switching Pt atom, i.e., the red curve.

additional single Pt atom. That Pt atom probes the nonlocality of the MAE following Eq. (7) by considering it along different directions and distances away from the magnetic adatom. In this investigation and to simplify the discussion, we do not include the NN atoms of that particular additional Pt atom in our cluster. Of course these boundary conditions will affect the final values of the nonlocal contributions but the general conclusions of this work are not affected. We perform two steps: in step 1 an SOI is switched on within the additional Pt atom. After removing the MAE of the Fe adatom and its three NN Pt atoms, we obtain the sum of the two terms given in Eq. (7). Then we proceed with step 2 and switch off the SOI, thereby getting the no-so-term, with which one extracts the so term to the sum in Eq. (7).

Figure 5 shows the nonlocal contributions from a single Pt atom as a function of the distance, d, from the adatom for *hcp* and *fcc* sites along two directions connecting the adatom to one of the Pt switching atoms. While in Fig. 5(a) we plot the sum of the nonlocal contributions, in Figs. 5(b) and 5(c) these contributions are resolved into the so and no-so terms for the *hcp* and *fcc* sites, respectively. In Figs. 5(a)–5(c), the chosen polar and azimuthal angles (θ, ϕ) are $(125°, -60°)$ (*hcp* stacking sites) and $(128°, 30°)$ (*fcc* stacking sites). Naturally, here we allow for an error bar for the angles ($\delta\theta = \pm 3°$ and $\delta\phi = \pm 8°$) since a straight line will not cross a sufficient number of Pt atoms at reasonable distances. One clearly sees that the sum of nonlocal terms is important outside the small inner region, with the largest contribution emanating from the switcher atom, which reaches a value of 0.37 meV for the Fe *fcc* site and 0.73 meV for the *hcp* site. As explained earlier, since there are only three switching atoms for the *fcc* site, instead of six for the *hcp* site, the barrier presented by the MAE of the adatom and its NNs is not overcome. When the distance from the adatom is increased, the induced term oscillates and even changes sign. Its magnitude, however, is not sufficient to overcome the aforementioned barrier. These oscillations as a function of the distance have a Friedel-like character and are similar to those obtained for long-ranged magnetic exchange interactions [35,48].

In Figs. 5(b) and 5(c), we note that the so term does not behave similarly to the no-so term. These two terms can counteract each other as for the contribution from the switcher atom. Thus, for this particular atom the so term is dominant and favors an in-plane orientation of the moment, in contrast to the no-so term. For large distances both terms oscillate nontrivially. Although the values plotted in Fig. 5 might look small at first glance, one should not forget that these are contributions from a single Pt atom. In the end, one has to sum up contributions from all the surrounding Pt atoms to get the full nonlocal part of the MAE.

These oscillating nonlocal parts of the MAE can be highly anisotropic as demonstrated in Fig. 5(d), where two directions are probed. The first is along the direction shown in Fig. 5(a), which connects the Fe adatom with one switcher atom, leading to a very large peak at 0.5 nm. The second probed direction does not cross such switcher atoms, and interestingly the calculated values are considerably smaller at short distances but show similar Friedel-like oscillations at long distances. Thus, the nonlocal MAE contribution from the outer Pt atoms shows Friedel-like oscillations but is highly anisotropic, which
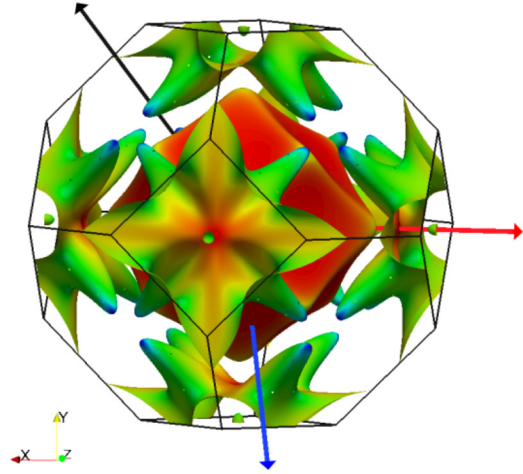

FIG. 6. Bulk Fermi surface of Pt, with the directions of probed atoms indicated by red and blue arrows and the [111] direction by a black arrow. The color code on the Fermi surface corresponds to the magnitude of the Fermi velocity (red and blue corresponding to high and low velocity, respectively).

is expected when looking at the Fermi surface of Pt presented in Fig. 6. Indeed the Fermi surface, extracted utilizing the scheme described in Ref. [50], is extremely anisotropic, such that isotropic oscillations resulting from a simple spherical Fermi surface are not expected in our particular system.

C. Case of Cr, Mn, and Co adatoms at *fcc* and *hcp* stacking sites

For completeness, we examined the impact of the Pt spin-polarization cloud on the MAE of Cr, Mn, and Co adatoms. Like the Fe adatom, the Co adatom and its NNs prefer an out-of-plane orientation of the magnetic moment independently of the binding site (Fig. 7). The MAE found in this case (-8.2 meV) is, however, higher than that of the Fe adatom, making the barrier higher for an in-plane reorientation of the magnetic moment when a large number of Pt substrate atoms (up to 221 atoms) is included. In addition, here the nonlocal contribution of the switching atoms to the MAE is even smaller than for the Fe adatom. The total MAE for the largest studied system decreases to -6.9 and -5.5 meV for the *hcp* and *fcc* sites, respectively. We point out that the experimental value of Gambardella *et al.* [1] is around -9 meV. This large value has generated a lot of theoretical investigations based on density functional theory. Usual simple exchange and correlation functionals, such as the local spin density approximation (LDA) or the generalized gradient approximation (GGA), leads to a rather low MAE. Therefore, correlation effects beyond the LDA or GGA were considered, e.g., by including a correlation U as a parameter or the orbital polarization scheme to tune the MAE and understand the origin of its large magnitude. Our work demonstrates that even without the invoked correlation effects, the nonlocal contribution to the MAE, not considered up to now, can be crucial in the case of Co as well. We predict that in the case of the *hcp* stacking site the MAE reaches approximately -7 meV.
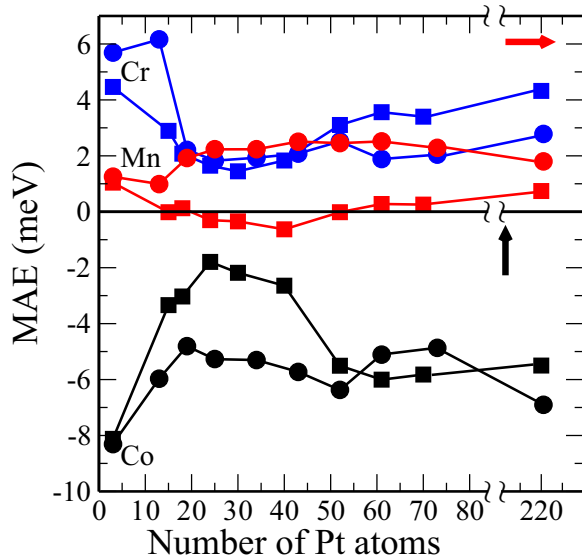
FIG. 7. The MAE of Co, Mn, and Cr impurities adsorbed at an *fcc* (squares) or at an *hcp* (circles) site on a Pt(111) surface versus the number of Pt atoms in the cluster. The convention of the sign of the MAE is identical to that used in Fig. 1.

The case of Mn is interesting since, contrary to what has been observed for Fe and Co, both the local and the nonlocal contributions to the MAE from the switching Pt atom favor an in-plane orientation of the magnetic moment. However, the rest of the Pt atoms are decisive. With an increase in their number, the adatom at the *fcc* binding site first switches to an out-of-plane magnetic orientation and then converges to an in-plane orientation. The Cr adatom behaves similarly to Mn, i.e., both the local and the nonlocal contributions to the MAE favor an in-plane orientation of the magnetic moment, but unlike Mn, the local term is large: +5.6 and +4.5 meV for the *hcp* and *fcc* stacking sites, respectively. Furthermore, compared to Mn, Fe, and Co adatoms, the switching atoms in the vicinity of the Cr adatom contribute to the MAE differently and favor an out-of-plane orientation of the moment. This contribution is, however, not large enough to overcome the barrier created by the adatom and its NNs. When the rest of the Pt atoms are included, Cr adatoms at both binding sites prefer an in-plane magnetic orientation.

When the chemical nature of the adatom is changed, the nonlocal behavior of the MAE is modified. As can be realized from Eq. (7), the scattering properties at the adatom site, described by T_1, can renormalize strongly the total MAE. T_1 depends obviously on the electronic properties of the adatom and its nearest surroundings. It is not a single number but a matrix, and therefore the trace in Eq. (7) is taken. Thus,

besides the impact on the magnitude of the MAE, nontrivial interference effects can occur, which affect the oscillating behavior of the MAE.

IV. DISCUSSION AND CONCLUSIONS

To summarize, for 3*d* adatoms on Pt(111) we have demonstrated the existence of long-range, RKKY-like, contributions to the MAE mediated by the electronic states of the substrate. Since they oscillate as a function of the distance with different kinds of decaying factors, they affect the magnitude of the total MAE and can even switch its sign. This depends on the details of the electronic structure, and as for Friedel oscillations or RKKY interactions, they can be highly anisotropic, with the possibility of observing a focusing effect induced by the shape of the constant-energy contours (e.g., the Fermi surface) [17,34,35,37]. Our results go beyond the approximations assumed according to our theoretical investigations. We expect non-negligible nonlocal contributions to the MAE independently of the assumptions related to the exchange and correlation functionals, geometrical relaxations, and inclusion of a U as done in the traditional LDA + U.

The established effect is expected to occur in other substrates with a high polarizability (e.g., Rh, W, Ir, Pd substrates), but also when confined electronic states are present in low-dimensional systems [e.g., surface states of Ag and Au(111) surfaces] since the latter favor a lower decay of the usual Friedel oscillations. We believe that this effect is active in the recently investigated surfaces of CuN/Cu(001) [8,51] and graphene/Rh(111) [52], where unusual behavior of the MAEs of different types of adsorbates has been observed. To verify experimentally the theoretical facts described in our work, one would, for example, have to switch off/on the spin-orbit interaction of a remote substrate Pt atom at will. This is certainly impossible, however, we believe that the signature of the nonlocality of the MAE could be detectable for two magnetic adatoms on a surface, for example, two Fe adatoms on a Pt(111) surface. We expect the MAE to be dependent on the interadatom distance, which is expect to be related to the nonlocal effect discussed in the text. Thus, we expect oscillatory behavior of the MAE measurable with state-of-the-art inelastic scanning tunneling spectroscopy, wherein the MAE leads to a gap in the excitation spectra.

[1] P. Gambardella, S. Rusponi, M. Veronese, S. S. Dhesi, C. Grazioli, A. Dallmeyer, I. Cabria, R. Zeller, P. H. Dederichs, K. Kern, C. Carbone, and H. Brune, Science **300**, 1130 (2003).

[2] M. Bode, O. Pietzsch, A. Kubetzka, and R. Wiesendanger, Phys. Rev. Lett. **92**, 067201 (2004).

[3] I. G. Rau, S. Baumann, S. Rusponi, F. Donati, S. Stepanow, L. Gragnaniello, J. Dreiser, C. Piamonteze, F. Nolting, S. Gangopadhyay, O. R. Albertini, R. M. Macfarlane, C. P. Lutz, B. A. Jones, P. Gambardella, A. J. Heinrich, and H. Brune, Science **344**, 988 (2014).

[4] A. A. Khajetoorians, S. Lounis, B. Chilian, A. T. Costa, L. Zhou, D. L. Mills, J. Wiebe, and R. Wiesendanger, Phys. Rev. Lett. **106**, 037205 (2011).

[5] Q. Dubout, F. Donati, C. Wäckerlin, F. Calleja, M. Etzkorn, A. Lehnert, L. Claude, P. Gambardella, and H. Brune, Phys. Rev. Lett. **114**, 106807 (2015).

[6] J. Honolka, T. Y. Lee, K. Kuhnke, A. Enders, R. Skomski, S. Bornemann, S. Mankovsky, J. Minár, J. Staunton, H. Ebert, M. Hessler, K. Fauth, G. Schütz, A. Buchsbaum, M. Schmid, P. Varga, and K. Kern, Phys. Rev. Lett. **102**, 067207 (2009).

[7] A. A. Khajetoorians, B. Baxevanis, C. Hübner, T. Schlenk, S. Krause, T. O. Wehling, S. Lounis, A. Lichtenstein, D. Pfannkuche, J. Wiebe, and R. Wiesendanger, Science **339**, 55 (2013).

[8] B. Bryant, A. Spinelli, J. J. T. Wagenaar, M. Gerrits, and A. F. Otte, Phys. Rev. Lett. **111**, 127203 (2013).

[9] S. Krause, L. Berbil-Bautista, G. Herzog, M. Bode, and R. Wiesendanger, Science **317**, 1537 (2007).

[10] P. Gambardella, A. Dallmeyer, K. Maiti, M. C. Malagoli, W. Eberhardt, K. Kern, and C. Carbone, Nature **416**, 301 (2002).

[11] R. Sessoli, D. Gatteschi, A. Caneschi, and M. A. Novak, Nature **365**, 141 (1993).

[12] D. Gatteschi, R. Sessoli, and J. Villain, *Molecular Nanomagnets* (Oxford University Press, Oxford, UK, 2006).

[13] J. Brede, N. Atodiresei, V. Caciuc, M. Bazarnik, A. Al-Zubi, S. Blügel, and R. Wiesendanger, Nature Nanotechnol. **9**, 1018 (2014).

[14] A. Lodi Rizzini, C. Krull, T. Balashov, J. J. Kavich, A. Mugarza, P. S. Miedema, P. K. Thakur, V. Sessi, S. Klyatskaya, M. Ruben, S. Stepanow, and P. Gambardella, Phys. Rev. Lett. **107**, 177205 (2011).

[15] A. A. Khajetoorians, T. Schlenk, B. Scheflinghaus, M. dos Santos Dias, M. Steinbrecher, M. Bouhassoune, S. Lounis, J. Wiebe, and R. Wiesendanger, Phys. Rev. Lett. **111**, 157204 (2013).

[16] O. Šipr, S. Bornemann, J. Minár, and H. Ebert, Phys. Rev. B **82**, 174414 (2010).

[17] F. Meier, S. Lounis, J. Wiebe, L. Zhou, S. Heers, Ph. Mavropoulos, P. H. Dederichs, S. Blügel, and R. Wiesendanger, Phys. Rev. B **83**, 075407 (2011).

[18] G. J. Nieuwenhuys, Adv. Phys. **24**, 515 (1975).

[19] T. Herrmannsdörfer, S. Rehmann, W. Wendler, and F. Pobell, J. Low Temp. Phys. **104**, 49 (1996).

[20] A. Oswald, R. Zeller, and P. H. Dederichs, Phys. Rev. Lett. **56**, 1419 (1986).

[21] K. Swieca, Y. Kondo, and F. Pobell, Phys. Rev. B **56**, 6066 (1997).

[22] S. Mitani, K. Takanashi, M. Sano, H. Fujimori, A. Osawa, and H. Nakajima, J. Magn. Magn. Mater. **148**, 163 (1995).

[23] P. Blonski, A. Lehnert, S. Dennler, S. Rusponi, M. Etzkorn, G. Moulas, P. Bencok, P. Gambardella, H. Brune, and J. Hafner, Phys. Rev. B **81**, 104426 (2010).

[24] L. Szunyogh and B. L. Gyorffy, Phys. Rev. Lett. **78**, 3765 (1997).

[25] L. Szunyogh, G. Zarand, S. Gallego, M. C. Munoz, and B. L. Gyorffy, Phys. Rev. Lett. **96**, 067204 (2006).

[26] C. J. Aas, K. Palotás, L. Szunyogh, and R. W. Chantrell, J. Phys.: Condens. Matter **24**, 406001 (2012).

[27] M. M. Sigalas and D. A. Papaconstantopoulos, Phys. Rev. B **50**, 7255 (1994).

[28] J. Friedel, Nuovo Cimento **7**, 287 (1958).

[29] M. A. Ruderman and C. Kittel, Phys. Rev. **96**, 99 (1954); T. Kasuya, Prog. Theor. Phys. **16**, 45 (1956); K. Yosida, Phys. Rev. **106**, 893 (1957).

[30] M. F. Crommie, C. P. Lutz, and D. M. Eigler, Nature **363**, 524 (1993).

[31] Y. Hasegawa and Ph. Avouris, Phys. Rev. Lett. **71**, 1071 (1993).

[32] L. Zhou, J. Wiebe, S. Lounis, E. Vedmedenko, F. Meier, P. H. Dederichs, S. Blügel, and R. Wiesendanger, Nat. Phys. **6**, 187 (2010).

[33] A. A. Khajetoorians, J. Wiebe, B. Chilian, S. Lounis, S. Blügel, and R. Wiesendanger, Nat. Phys. **8**, 497 (2012).

[34] A. Weismann, M. Wenderoth, S. Lounis, P. Zahn, N. Quaas, R. G. Ulbrich, P. H. Dederichs, and S. Blügel, Science **323**, 1190 (2009).

[35] S. Lounis, P. Zahn, A. Weismann, M. Wenderoth, R. G. Ulbrich, I. Mertig, P. H. Dederichs, and S. Blügel, Phys. Rev. B **83**, 035427 (2011).

[36] Ye. S. Avotina, Yu. A. Kolesnichenko, A. N. Omelyanchouk, A. F. Otte, and J. M. van Ruitenbeek, Phys. Rev. B **71**, 115430 (2005).

[37] M. Bouhassoune, B. Zimmermann, Ph. Mavropoulos, D. Wortmann, P. H. Dederichs, S. Blügel, and S. Lounis, Nature Commun. **5**, 5558 (2014).

[38] H. Prüser, P. E. Dargel, M. Bouhassoune, R. G. Ulbrich, T. Pruschke, S. Lounis, and M. Wenderoth, Nature Commun. **5**, 5417 (2014).

[39] S. Lounis, A. Bringer, and S. Blügel, Phys. Rev. Lett. **108**, 207202 (2012).

[40] A. R. Mackintosh and O. K. Andersen, in *Electron at the Fermi Surface*, edited by M. Springford (Cambridge University Press, Cambridge, UK, 1980), p. 149.

[41] H. J. F. Jansen, Phys. Rev. B **59**, 4699 (1999).

[42] N. Papanikolaou *et al.*, J. Phys.: Condens. Matter **14**, 2799 (2002).

[43] D. Bauer, Ph.D. thesis, Forschungszentrum Jülich and RWTH Aachen, 2014.

[44] S. Vosko, L. Wilk, and M. Nusair, Can. J. Phys. **58**, 1200 (1980).

[45] P. Blonski and J. Hafner, J. Phys.: Condens. Matter **21**, 426001 (2009).

[46] B. Scheflinghaus, M. dos Santos Dias, and S. Lounis, Phys. Rev. B **93**, 035451 (2016).

[47] P. Lloyd, Proc. Phys. Soc. **90**, 207 (1967).

[48] A. I. Liechtenstein, M. I. Katsnelson, V. P. Antropov, and V. A. Gubanov, J. Magn. Magn. Mater. **67**, 65 (1987).

[49] S. Lounis and P. H. Dederichs, Phys. Rev. B **82**, 180404(R) (2010).

[50] B. Zimmermann, Ph. Mavropoulos, N. H. Long, C.-R. Gerhorst, S. Blügel, and Y. Mokrousov, Phys. Rev. B **93**, 144403 (2016).

[51] J. C. Oberg, M. R. Calvo, F. Delgado, M. Moro-Lagares, D. Serrate, D. Jacob, J. Fernandez-Rossier, and C. F. Hirjibehedin, Nature Nano. **9**, 64 (2014).

[52] P. Jacobson, T. Herden, M. Muenks, G. Laskin, O. Brovko, V. Stepanyuk, M. Ternes, and K. Kern, Nature Comm. **6**, 8536 (2015).